Information Sciences Letters
An International Journal

http://dx.doi.org/10.12785/isl/030203

Theoretical Investigation of MHD Nanofluid Flow Over a Rotating Cone: An Optimal Solutions

*S. Nadeem and S. Saleem**

Department of Mathematics, Quaid-i-Azam University 45320, Islamabad 44000, Pakistan

Received: 9 Dec. 2013, Revised: 18 Mar. 2014, Accepted: 19 Mar. 2014
Published online: 1 May 2014

Abstract: The problem of MHD nanofluid flow over a rotating cone in the presence of thermal radiation has been investigated. The model used for the nanofluid includes the effects of Brownian motion and thermophoresis with Rosseland diffusion approximation. The governing nonlinear partial differential equations have been treated analytically by using optimal homotopy analysis method. A parametric study of various emerging parameters are presented for velocity, temperature, nano particle volume fraction, Skin friction coefficients, Nusselt and Sherwood numbers in graphical and tabular form. The comparison of present results with the numerical results available in literature is made and our results are in very suitable agreement with the known results. Also, the main features of the observations are examined and deliberated.

Keywords: Nanofluids, Heat transfer analysis, Thermal radiation, Optimal solutions.

1 Introduction

The phenomena of flows over rotating bodies earned countless consideration because of their occurrence in turbines and turbo machines, in gaseous and nuclear reactors, in approximating the conduit of flight of spinning wheels in the modeling of several geophysical vortices. The magnetohydrodynamics of rotating electrically conducting fluids in the presence of the magnetic field finds uses in geophysics and astrophysics. The preservation and secular differences of the geomagnetic field [1]. Solar cycle and the configuration of rotating magnetic stars are too a remarkable study. It is practically seen that whenever some rotating flow collaborates through a surface, a three dimensional complex flow exists which appear in both outward and interior flows. Also the probability of cooling the nose-cone of re-entry vehicles by rotating the nose is an important application [2]. The flow over an infinite rotating disk in an ambient fluid was first deliberated by Von Karman [3]. The influence of the MHD on the rotating infinite disk in an ambient fluid was studied by Sparrow and Cess [4] and Tarek et al. [5]. Initially Dorffman [6] and Krieth [7] investigate the flow and heat transfer in rotating systems. Hartnett and Deland [8] examined the effects of Prandtl number on the heat transfer by rotating bodies. Heiring and Grosh [9] have reported the mixed convection by a rotational non-isothermal cone at low Prandtl number. Himasekhar et al. [10] presents the study of the similarity solution of the mixed convection flow over a vertical rotating cone in a fluid for a wide range of Prandtl numbers. Vira and Fan [11] have examined the flow and heat transfer on a rotating cone in a rotating fluid. Boundary layers on rotating cone, disc and axisymmetric surfaces with a concentrated heat sources have been reported by Wang [12]. An approximate method of solution for the heat transfer from vertical cones in laminar natural convection was examined by Alamgir [13]. The laminar steady non-similar natural convection flow of gases over an isothermal vertical cone has been studied by Takhar et al. [14]. The above cited works are associated to steady and axi-symmetric flows. On the other hand in many real world problems the flows are time dependent. Ece [15] reported the time dependent boundary layer flow of an impulsively started translating a spinning rotational symmetric body. Later on Anilkumar and Roy [16] studied the unsteady mixed convection from a rotating cone in a rotating fluid with thermal and mass diffusion. MHD heat and mass transfer from a rotating vertical cone with heat generation or absorption effects was presented by Chamkha et al. [17].

* Corresponding author e-mail: salmansaleem_33@hotmail.com

It is evident that convective heat transfer fluids, containing oil, water and ethylene glycol mixture are not highly heat transfer fluids, as there is a vital contribution of thermal conductivity of these fluids on the coefficient of heat transfer among the heat transfer medium and the heat transfer surface. Ultra-fine solid particles are broadly used for improving the heat transfer in the fluids from last rare years [18,19,20]. The theory of convective heat transfer in nanofluids takes an excessive concern for investigators lately due to the reports of impressively higher thermal properties. Primarily Choi [20] familiarized the word nanofluid, which is a base fluid with suspended metallic nano-size particles specifically nano particles with sizes typically of 1-100nm [21]. If inveterate and found consistent, nanofluid finds application in thermal management. Suspended metal nano particles are likewise settled for other physical phenomena's, for example cancer therapy. The nanofluids are extensively used as coolants, lubricants, heat exchangers and micro-channel heat sinks. The interdisciplinary behavior of nanofluid study gives a great chance for study and innovation at the frontlines of nanotechnology. Chamkha et al. [22] gives a study of natural convection past a sphere embedded in a porous medium saturated by a nanofluid. Some of the studies of nanofluids are given in refs. [19,20,21,22,23,24,25,26,27,28,29,30,31].

The motivation of the present analysis is to investigate the radiative boundary layer flow over a rotating cone in a nanofluid with magnetic effects. The coupled nonlinear parabolic partial differential equations governing the unsteady flow have been solved analytically by using optimal homotopy analysis method [32,33,34,35,36]. A parametric study of various parameters are presented in graphical and tabular form. Also the comparison of present results with the numerical results available in literature is given as a special case of the present study.

2 Mathematical formulation

We have considered the unsteady incompressible electrically conducting fluid flow over a rotating cone in a viscous fluid with nanoparticles. The cone is rotating with time-dependent angular velocity about the axis of symmetry. The non-rotating curvilinear coordinate system is given in figure 1, where x is taken along a meridional section, the y-axis along a circular section and the z-axis normal to the surface of cone. It is assumed that u, v and w be the velocity components in tangential, azimuthal and normal directions, respectively. The wall temperature T_w and wall nano particle volume fraction C_w are linear functions of distance x and the free stream temperature T_∞ and nano particle volume fraction C_∞ are constant. The time dependent angular velocity Ω_0 of the cone causes the unsteadiness in the flow field. The surface of cone is taken to be electrically insulated. The magnetic field $\mathbf{B}_0$ is applied in z-direction. The magnetic Reynolds number is

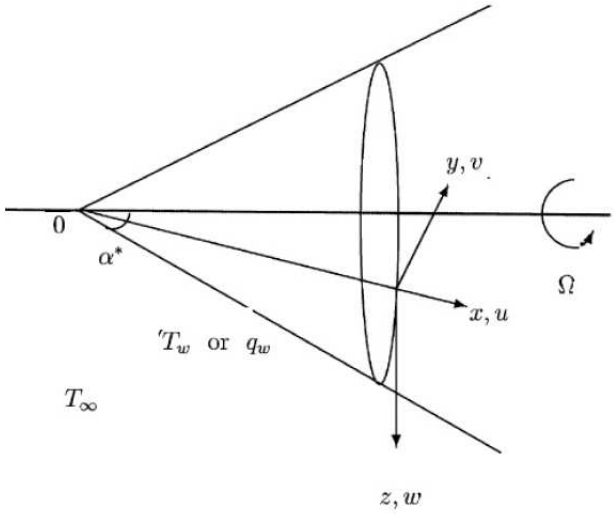

Fig. 1: Schematic diagram of the physical model and coordinate system.

assumed to be small $Re_m = \mu_0 \sigma V L \ll 1$ where μ_0, σ, V and L are the magnetic permeability, the electrical conductivity, characteristic velocity and the length, respectively. Under such expectations, we neglect the induced magnetic field. As the flow is not executed by the applied or polarization of voltage, the electric field $\mathbf{E} = 0$. Hence only the applied magnetic field contributes towards the Lorentz force. Moreover axi-symmetric nature of flow is considered and the pressure gradient and viscous dissipation effects are neglected.

The boundary layer equations for flow, heat and mass transfer over a rotating cone in a nanofluid are listed as

$$\frac{1}{x}\frac{\partial(xu)}{\partial x} + \frac{\partial(w)}{\partial z} = 0, \tag{1}$$

$$\frac{\partial u}{\partial t} + u\frac{\partial u}{\partial x} + w\frac{\partial u}{\partial z} - \frac{v^2}{x} = \nu\frac{\partial^2 u}{\partial z^2} - \frac{\sigma}{\rho}B^2 u, \tag{2}$$

$$\frac{\partial v}{\partial t} + u\frac{\partial v}{\partial x} + w\frac{\partial v}{\partial z} + \frac{uv}{x} = \nu\frac{\partial^2 v}{\partial z^2} - \frac{\sigma}{\rho}B^2 v, \tag{3}$$

$$\frac{\partial T}{\partial t} + u\frac{\partial T}{\partial x} + w\frac{\partial T}{\partial z} = \frac{\kappa_0}{\rho c_f}\frac{\partial^2 T}{\partial z^2} - \frac{1}{\rho c_f}\frac{\partial q_r}{\partial t} + \tau\left[D_B\frac{\partial C}{\partial z}\frac{\partial T}{\partial z} + \frac{D_T}{T_\infty}\left(\frac{\partial T}{\partial z}\right)^2\right], \tag{4}$$

$$\frac{\partial C}{\partial t} + u\frac{\partial C}{\partial x} + w\frac{\partial C}{\partial z} = D_B\frac{\partial^2 C}{\partial z^2} + \frac{D_T}{T_\infty}\frac{\partial^2 T}{\partial z^2} \tag{5}$$

The boundary conditions applicable for problem are given by [17]

$$u(x,0,t) = w(x,0,t) = 0,\ v(x,0,t) = \Omega_0 x \sin\alpha^* R(t^*)$$

$$T(x,0,t) = T_w,\ C(x,0,t) = C_w$$
$$u(x,\infty,t) = 0,\ v(x,\infty,t) = 0$$
$$T(x,\infty,t) = T_\infty,\ C(x,\infty,t) = C_\infty \quad (6)$$

Here ρ is the density, t and $t^*(=\Omega\sin\alpha^* t)$ are the dimensional and dimensionless times, respectively, α^* is the semi-vertical angle of the cone, υ is the kinematic viscosity, Ω_0 is the angular velocity of the cone, T is the temperature,C is the species concentration, κ_0 is the thermal conductivity of the fluid, q_r is the radiative heat flux, τ is the ratio of nano particle heat capacity and the base fluid heat capacity, D_B is the Brownian diffusion coefficient and D_T is the thermophretic diffusion coefficient, the subscripts w and ∞ denote the conditions at the wall and the ambient conditions, respectively. By using the Rosseland approximation $q_r = -\frac{4\sigma^*}{3\kappa^*}\frac{\partial T^4}{\partial z}$ in which σ^* denotes the Stefan–Boltzman constant and κ^* the Rosseland mean absorption coefficient. The fluid phase temperature differences within the flow are sufficiently small so that T^4 may be described as a linear function of temperature. Hence, expanding T^4 in Taylors series about the free-stream temperature T_∞ and neglecting higher order terms, we have $T^4 \approx 4T_\infty^3 T - 3T_\infty^4$. Invoking these in Eq. 4 we may write

$$\frac{\partial T}{\partial t} + u\frac{\partial T}{\partial x} + w\frac{\partial T}{\partial z} = \left(\frac{\kappa_0}{\rho c_f} + \frac{16\sigma^* T_\infty^3}{3\rho c_f \kappa^*}\right)\frac{\partial^2 T}{\partial z^2} + \tau[D_B\frac{\partial C}{\partial z}\frac{\partial T}{\partial z} + \frac{D_T}{T_\infty}(\frac{\partial T}{\partial z})^2]. \quad (7)$$

We now reduce the number of independent variables in Eqs. $(1)-(5)$ from three (x,z,t) to two (η,t^*) with the help following transformations.

$$\begin{aligned}
\eta &= \left(\frac{\Omega_0\sin\alpha^*}{\nu}\right)^{\frac{1}{2}} z,\ t^*(=\Omega\sin\alpha^* t),\ u(x,z,t)\\
&= -2^{-1}(\Omega_0 x\sin\alpha^*)R(t^*)h'(\eta,t^*),\\
v(x,z,t) &= (\Omega_0 x\sin\alpha^*)R(t^*)g(\eta,t^*),\\
w(x,z,t) &= (\nu\Omega_0\sin\alpha^*)^{\frac{1}{2}}R(t^*)h(\eta,t^*),\\
T(x,z,t)-T_\infty &= (T_w-T_\infty)\theta(\eta,t^*),\ T_w-T_\infty = (T_0-T_\infty)\left(\frac{x}{L}\right),\\
C(x,z,t)-C_\infty &= (C_w-C_\infty)\phi(\eta,t^*),\ (C_w-C_\infty) = (C_0-C_\infty)\left(\frac{x}{L}\right),\\
R(t^*) &= 1+\varepsilon t^*,\ \mathrm{Pr} = \frac{\nu}{\alpha},\ Le = \frac{\alpha}{D_M},\\
Nb &= \frac{(\rho c)_p D_B(C_w-C_\infty)}{\nu(\rho c)_f},\ M = \frac{\sigma B_0^2}{\rho}(\Omega_0\sin\alpha^*)^{-1}\\
Nt &= \frac{(\rho c)_p D_T(T_w-T_\infty)}{\nu(\rho c)_f T_\infty},\ Le = \frac{\nu}{D_B},\ k = \frac{4\sigma^* T_\infty^3}{\kappa^*\kappa_0}.
\end{aligned} \quad (8)$$

The above transformations satisfies the continuity equation i.e Eq. (1) and Eqs. $(2)-(5)$ are stated as

$$h''' - R(t^*)hh'' + \tfrac{1}{2}R(t^*)(h')^2 - 2R(t^*)g^2 - \tfrac{1}{R(t^*)}\tfrac{dR}{dt^*}h' - \tfrac{\partial h'}{\partial t^*} - Mh' = 0, \quad (9)$$

$$g'' + R(t^*)\left(gh' - hg'\right) - \left(M + \frac{1}{R(t^*)}\frac{dR}{dt^*}\right)g - \frac{\partial g}{\partial t^*} = 0, \quad (10)$$

$$(1+\tfrac{4}{3}k)\theta'' - \mathrm{Pr}\left\{R(t^*)\left(h\theta' - h'\tfrac{\theta}{2}\right) - \tfrac{\partial\theta}{\partial t^*} + Nb\phi'\theta' + Nt\theta'^2\right\} = 0, \quad (11)$$

$$\phi'' - Le\left\{R(t^*)\left(h\phi' - h'\frac{\phi}{2}\right) + \frac{\partial\phi}{\partial t^*}\right\} + \frac{Nt}{Nb}\theta'' = 0. \quad (12)$$

The boundary conditions take the form

$$\begin{aligned}
&\text{When } \eta \to 0 : h(\eta,t^*) = 0 = h'(\eta,t^*),\ g(\eta,t^*) = 1,\ \theta(\eta,t^*) = \phi(\eta,t^*) = 1,\\
&\text{as } \eta \to \infty : h'(\eta,t^*) = 0,\ g(\eta,t^*) = 0,\ \theta(\eta,t^*) = \phi(\eta,t^*) = 0,
\end{aligned} \quad (13)$$

where Nb is the Brownian motion parameter , Nt is the Thermophoresis parameter and Le is the Lewis number, k is the radiation number, M is the dimensionless magnetic parameter and prime denotes the derivative with respect to η. The dimensionless local surface skin friction coefficients in tangential and azimuthal directions, the local Nusselt number and local Sherwood number are given as where Nb is the Brownian motion parameter , Nt is the Thermophoresis parameter and Le is the Lewis number, k is the radiation number, M is the dimensionless magnetic parameter and prime denotes the derivative with respect to η. The dimensionless local surface skin friction coefficients in tangential and azimuthal directions, the local Nusselt number and local Sherwood number are given as

$$\begin{aligned}
C_{fx}Re_x^{\frac{1}{2}} &= \frac{2\mu(\frac{\partial u}{\partial z})\Big|_{z=0}}{\rho(\Omega_0 x\sin\alpha^*)^2} = -R(t^*)h''(0,t^*),\\
2^{-1}C_{fy}Re_x^{\frac{1}{2}} &= -\frac{2\mu(\frac{\partial v}{\partial z})\Big|_{z=0}}{\rho(\Omega_0 x\sin\alpha^*)^2} = -R(t^*)g'(0,t^*),
\end{aligned} \quad (14)$$

$$\begin{aligned}
Nu &= -\frac{\left[x\left(\frac{\partial T}{\partial z}\right)\right]_{z=0}}{T_w - T\infty} = -Re_x^{\frac{1}{2}}\theta'(0,t^*),\\
Sh &= -\frac{\left[x\left(\frac{\partial C}{\partial z}\right)\right]_{z=0}}{C_w - C\infty} = -Re_x^{\frac{1}{2}}\phi'(0,t^*),
\end{aligned} \quad (15)$$

where $Re_x = \frac{\Omega_0 x^2\sin\alpha^*}{\nu}$ is the local Reynolds number.

3 Homotopy analysis method

The initial approximations h_0, g_0, θ_0 and ϕ_0 with the respective auxiliary linear operators for the HAM solutions are

$$h_0(\eta,t^*) = 0, \quad (16)$$

$$g_0(\eta,t^*) = \exp(-\eta), \quad (17)$$

$$\theta_0(\eta,t^*) = \exp(-\eta), \quad (18)$$

$$\phi_0(\eta,t^*) = \exp(-\eta), \quad (19)$$

$$\iota_h = \frac{\partial^3 h(\eta,t^*)}{\partial\eta^3} - \frac{\partial h(\eta,t^*)}{\partial\eta}, \quad (20)$$

$$\iota_g = \frac{\partial^2 g(\eta,t^*)}{\partial \eta^2} + \frac{\partial g(\eta,t^*)}{\partial \eta}, \tag{21}$$

$$\iota_\theta = \frac{\partial^2 \theta(\eta,t^*)}{\partial \eta^2} + \frac{\partial \theta(\eta,t^*)}{\partial \eta}, \tag{22}$$

$$\iota_\phi = \frac{\partial^2 \phi(\eta,t^*)}{\partial \eta^2} + \frac{\partial \phi(\eta,t^*)}{\partial \eta}. \tag{23}$$

Some studies on the method are presented in [32,33,34, 35,36].

4 Optimal convergence-control parameters

It is seen that the HAM solutions, contain the non-zero auxiliary parameters c_0^h, c_0^g, c_0^θ and c_0^ϕ, which are used to find the convergence-region and rate of the homotopy series solutions. In order to determine the optimal values of c_0^h, c_0^g, c_0^θ and c_0^ϕ it is used here the so-called average residual error defined by [33].

$$\varepsilon_m^h = \frac{1}{k+1}\sum_{j=0}^{k}\left[\mathscr{N}_h(\sum_{i=0}^{m}\hat{h}(\eta,t^*),\sum_{i=0}^{m}\hat{g}(\eta,t^*))_{y=j\delta y}\right]^2 dy \tag{24}$$

$$\varepsilon_m^g = \frac{1}{k+1}\sum_{j=0}^{k}\left[\mathscr{N}_g(\sum_{i=0}^{m}\hat{h}(\eta,t^*),\sum_{i=0}^{m}\hat{g}(\eta,t^*))_{y=j\delta y}\right]^2 dy \tag{25}$$

$$\varepsilon_m^\theta = \frac{1}{k+1}\sum_{j=0}^{k}\left[\mathscr{N}_\theta(\sum_{i=0}^{m}\hat{h}(\eta,t^*),\sum_{i=0}^{m}\hat{\theta}(\eta,t^*),\sum_{i=0}^{m}\hat{\phi}(\eta,t^*))_{y=j\delta y}\right]^2 dy \tag{26}$$

$$\varepsilon_m^\phi = \frac{1}{k+1}\sum_{j=0}^{k}\left[\mathscr{N}_\phi(\sum_{i=0}^{m}\hat{h}(\eta,t^*),\sum_{i=0}^{m}\hat{\theta}(\eta,t^*),\sum_{i=0}^{m}\hat{\phi}(\eta,t^*))_{y=j\delta y}\right]^2 dy \tag{27}$$

Following Liao [33]

$$\varepsilon_m^t = \varepsilon_m^h + \varepsilon_m^g + \varepsilon_m^\theta + \varepsilon_m^\phi \tag{28}$$

where ε_m^t is the total squared residual error, $\delta y = 0.5$, $k = 20$. Total average squared residual error is minimized by using symbolic computation software Mathematica. We have directly applied the command **Minimize** to obtain the corresponding local optimal convergence control parameters. Tables 1 and 2 are displayed for the case of single optimal convergence control parameter. It is found that the averaged squared residual errors and total averaged squared residual errors are reduces as the order of approximation increases. Therefore, Optimal Homotopy Analysis Method gives us a great choice to select any set of local convergence control parameters to obtain convergent results.

Table 1: Total Averaged squared residual errors using single optimal convergence control parameters.

m	c_0	ε_m^t
5	-0.56	1.02×10^{-3}
10	-0.63	4.19×10^{-4}
15	-0.50	3.03×10^{-4}

Table 2: Average squared residual errors using Table 1.

m	5	10	15
ε_m^h	2.00×10^{-4}	5.64×10^{-7}	1.68×10^{-7}
ε_m^g	2.67×10^{-5}	1.46×10^{-6}	6.55×10^{-8}
ε_m^θ	5.58×10^{-4}	1.28×10^{-4}	1.11×10^{-5}
ε_m^ϕ	2.39×10^{-4}	2.20×10^{-4}	2.11×10^{-4}

5 Graphical results and discussion

The governing nonlinear boundary layer partial differential equations $(9)-(12)$ along with the boundary conditions (13) are solved by optimal homotopy analysis method. The graphical and numerical results of non-dimensional velocities, temperature, nano particle volume fraction, Skin friction coefficients, Nusselt and Sherwood numbers are computed for magnetic parameter M, Radiation parameter κ, Prandtl number Pr, Brownian motion parameter Nb, Thermophoresis parameter Nt and Lewis number Le. The influence of magnetic parameter M on the velocity $-h'(\eta,t^*)$ is presented in Fig. 2. It is depicted from the respective figure that the increase in M decreases the velocity and the boundary layer thickness. The velocity $g(\eta,t^*)$ shows the similar behavior as that of velocity $-h'(\eta,t^*)$ for M (see Fig. 3). Figs. 4 and 5 are plotted to see the influence of magnetic parameter M on the local Skin friction coefficients in tangential and azimuthal directions ($C_{fx}Re_x^{\frac{1}{2}}$, $0.5C_{fy}Re_x^{\frac{1}{2}}$) for increasing and decreasing angular velocity $R(t^*)$ respectively. It is seen from the Figs. 4 and 5 that $C_{fx}Re_x^{\frac{1}{2}}$ decreases by an increase in the values of M for both increasing and decreasing angular velocity but $0.5C_{fy}Re_x^{\frac{1}{2}}$ shows an increasing variation. The magnetic field induces a magnetic force in the tangential direction which inclines to directly oppose $-h'(\eta,t^*)$, therefore the values of $-h'(\eta,t^*)$ is reduced with increasing M and the tangential velocity gradient is also decreased with increasing M. On the other side, the non dimensional velocity $g(\eta,t^*)$ is an increasing function of M as the magnetic force induced by the magnetic field supports the motion. This causes in an increase in the skin friction coefficient in the azimuthal direction $0.5C_{fy}Re_x^{\frac{1}{2}}$. Meanwhile an increase in the angular velocity with time directly affects the tangential and azimuthal velocity components, the skin friction coefficients are expressively affected. But, the influence of an increase in the angular velocity on the energy and concentration equations are

Table 3: Comparison of OHAM results and numerical results when $k = t^* = \lambda = Nb = Nt = 0$

OHAM results			Chamkha et.al [17]	
M	$-h''(0)$	$-g'(0)$	$-h''(0)$	$-g'(0)$
0	1.0207	0.6158	1.0207 1.0210*	0.6159 0.6160*
0.5	0.7703	0.8488	0.773 0.7700*	0.8488 0.8490*
1	0.6190	1.0692	0.6194 0.6190*	1.0692 1.0690*
2	0.4611	1.4418	0.4613 0.4610*	1.4418 1.4420*
3	0.3813	1.7477	0.3813 0.3810*	1.7477 1.7480*
1	0.3308	2.0097	0.3308 0.3310*	2.0097 2.0100*

slightly indirect. Fig. 6 elucidate the effect of radiation parameter κ on temperature field $\theta(\eta,t^*)$. It is inspected from the figure that $\theta(\eta,t^*)$ increases for κ. The temperature and the thermal boundary layer thickness decreases with an increasing values of Prandtl number Pr. The reason behind this is that greater Prandtl number Pr fluid has a lower thermal conductivity which results in thinner thermal boundary layer and therefore the rate of heat transfer rate increases. For engineering point of view, the heat transfer rate should be low. This can be achieved by keeping the low temperature difference between the surface and the free stream fluid, using a low Prandtl number fluid, maintaining the surface at a constant temperature instead of at a constant heat flux. The effects of Brownian motion parameter Nb on the temperature $\theta(\eta,t^*)$ and the nano particle volume fraction $\phi(\eta,t^*)$ is shown in Figs. 8 and 9 respectively. The behavior is found to be opposite for both the fields. It is illustrated from Figs. 10 and 11 that the Thermophoresis parameter Nt increases both the temperature as well as the nano particle volume fraction respectively. Figs. 12 and 13 predicts that Lewis number Le causes an increase in temperature $\theta(\eta,t^*)$ while decreases the nano particle volume fraction $\phi(\eta,t^*)$. Table 3 and 4 are the comparison tables computed for OHAM results with the Numerical results [5,17]. It is obvious from the tables that there is a decent agreement between the OHAM and numerical results. The tabular values of local Nusselt number and local Sherwood number for Prandtl number Pr, radiation parameter κ and nano parameters are computed in table 5. It is found that local Nusselt number is a decreasing function of κ, Nb, Nt and Le. whereas for Prandtl number it reveres its trend. Further the local Sherwood number increases for Pr, Le and Nb but decreases for Nt and κ.

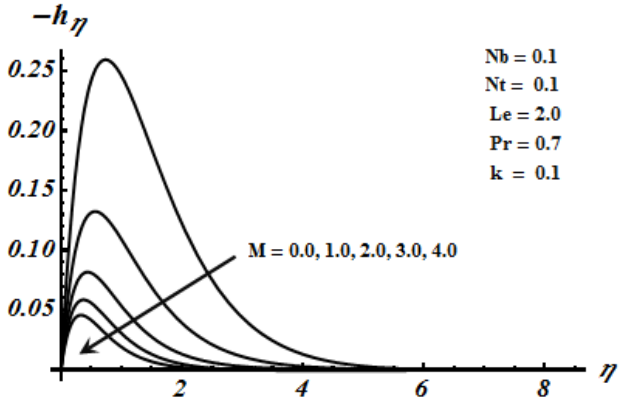

Fig. 2: effects of M on tangential velocity $-h'(\eta,t^*)$ when $R(t^*) = 1+\varepsilon t^*$, $\varepsilon = 0.2$ at $t^* = 1$

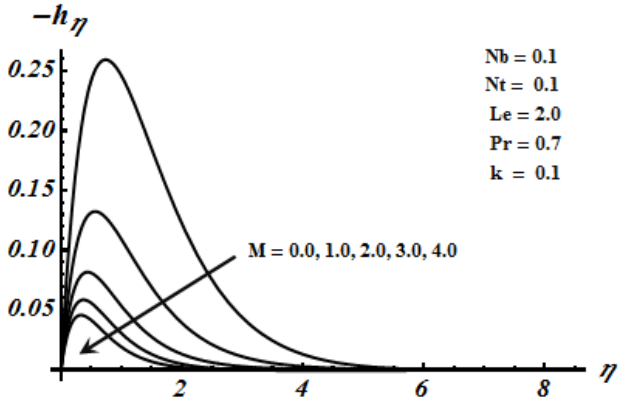

Fig. 3: effects of M on Azimuthal velocity $g(\eta,t^*)$ when $R(t^*) = 1+\varepsilon t^*$, $\varepsilon = 0.2$ at $t^* = 1$

Table 4: Comparison of OHAM results and numerical results when $k = t^* = \lambda = Nb = Nt = 0$ $*$Values taken from Sparrow and Cess [4]

OHAM results			Chamkha et.al [17]	
$\downarrow Pr, \mathbf{M}$	0.1	1	0.1	1
0.5	0.0426	0.2819	0.0426 0.0428	0.2819 0.282*
1	0.0281	0.1937	0.0282 0.0244	0.1939 0.194*
2	0.0105	0.0981	0.0107 0.0108	0.0981 0.0982*
3	0.00612	0.0585	0.00612 0.00614	0.0587 0.0588*
4	0.00400	0.0346	0.00406 0.00407	0.0344 0.0395*

6 Conclusions

The present work is the study of MHD boundary layer flow on a rotating cone in a rotating nanofluid with radiative effects. The reduced partial differential equations are treated by optimal homotopy analysis method. Magnetic parameter M decreases the velocity in the primary as well as in the secondary direction. The thermal boundary layer increases for increasing values for

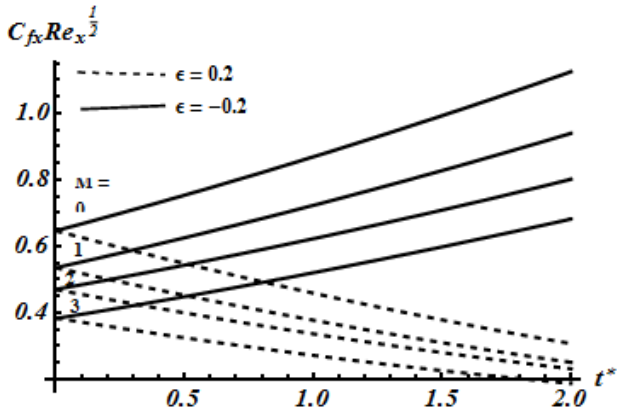

Fig. 4: effects of M on tangential Skin friction coefficient $C_{fx}Re_x^{\frac{1}{2}}$

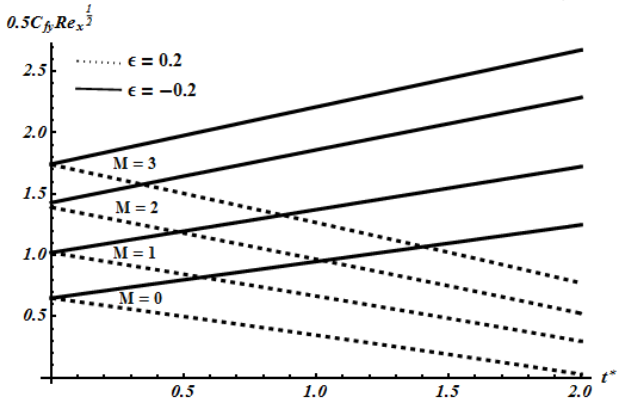

Fig. 5: effects of M on Azimuthal Skin friction coefficient $C_{fy}Re_x^{\frac{1}{2}}$

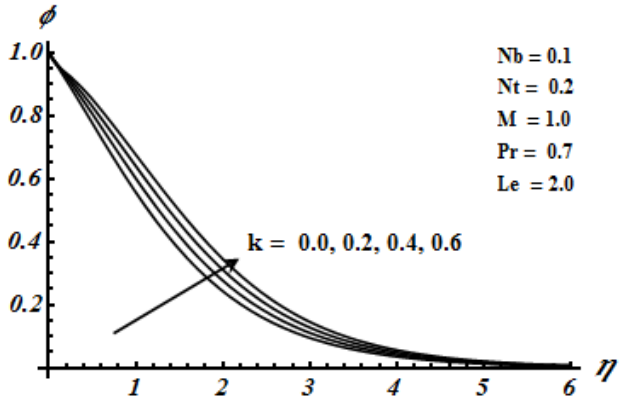

Fig. 6: effects of k on temperature field $\theta(\eta,t^*)$ when $R(t^*) = 1+\varepsilon t^*$, $\varepsilon = 0.2$ at $t^* = 1$

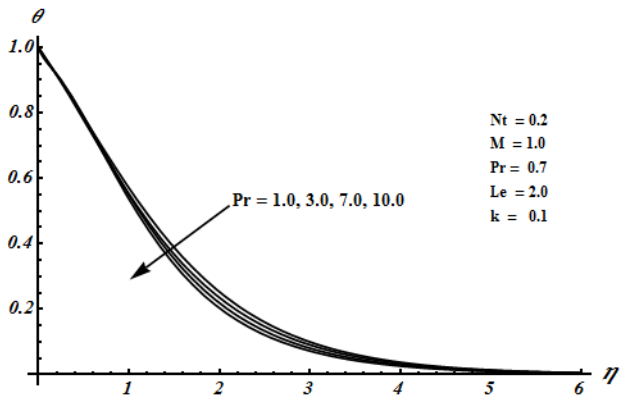

Fig. 7: effects of Pr on temperature field $\theta(\eta,t^*)$ when $R(t^*) = 1+\varepsilon t^*$, $\varepsilon = 0.2$ at $t^* = 1$

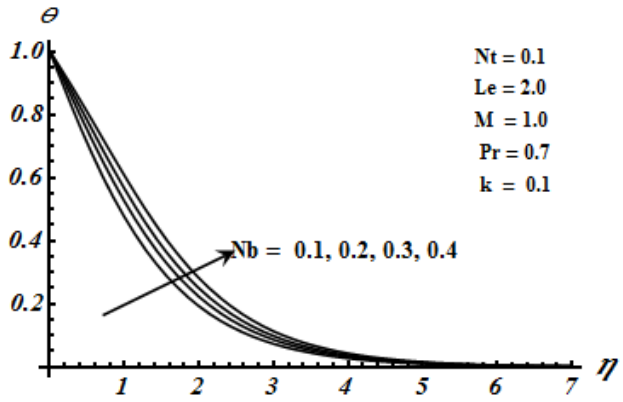

Fig. 8: effects of Nb on temperature field $\theta(\eta,t^*)$ when $R(t^*) = 1+\varepsilon t^*$, $\varepsilon = 0.2$ at $t^* = 1$

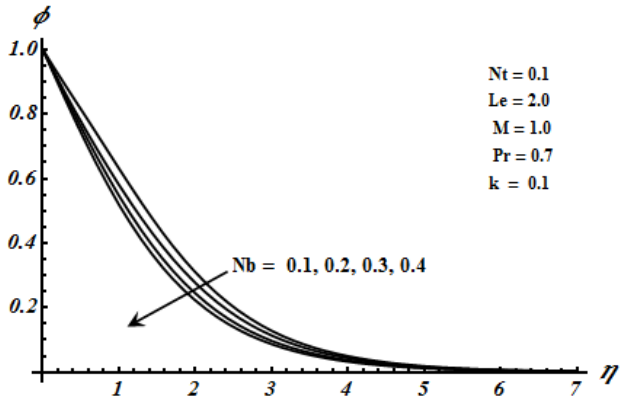

Fig. 9: effects of Nb on nano particle volume fraction $\phi(\eta,t^*)$ when $R(t^*) = 1+\varepsilon t^*$, $\varepsilon = 0.2$ at $t^* = 1$

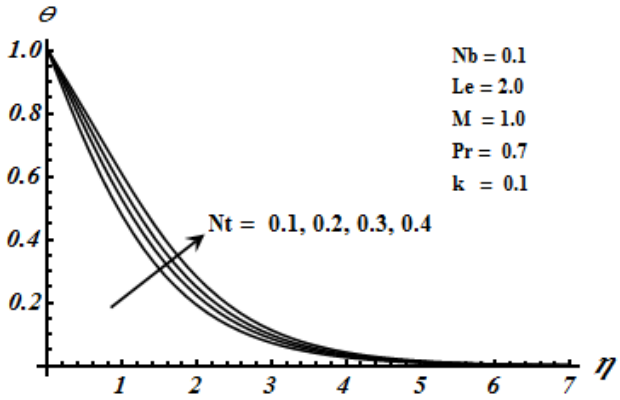

Fig. 10: effects of Nt on temperature field $\theta(\eta,t^*)$ when $R(t^*)=1+\varepsilon t^*$, $\varepsilon=0.2$ at $t^*=1$

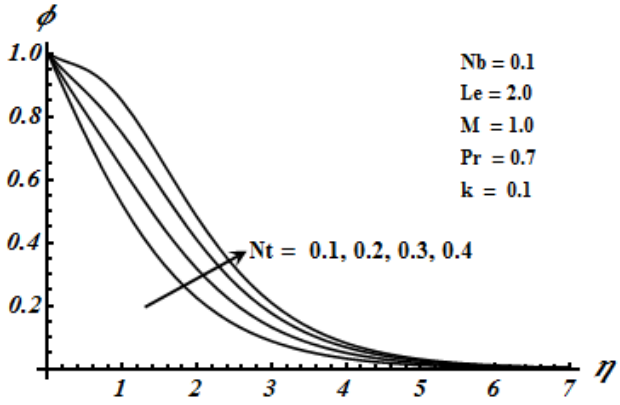

Fig. 11: effects of Nb on nano particle volume fraction $\phi(\eta,t^*)$ when $R(t^*)=1+\varepsilon t^*$, $\varepsilon=0.2$ at $t^*=1$

Table 5: Numerical variation of local Nusselt number and local Sherwood number for different emerging parameters

Pr	Le	Nb	Nt	k	$-\theta'(0)$	$-\phi'(0)$
2.0					1.01316	0.59033
3.0					1.32795	0.60863
4.0					1.66688	0.62706
	1.0				0.51703	0.38328
	2.0				0.51637	0.44999
	3.0				0.51571	0.51622
		0.2			0.46384	0.56097
		0.4			0.43489	0.60411
		0.6			0.40716	0.61833
			0.2		0.46825	0.33016
			0.4		0.44800	0.10379
			0.6		0.42873	−0.05937
				0.3	0.61215	0.61215
				0.6	0.58345	0.58834
				0.9	0.57343	0.57343

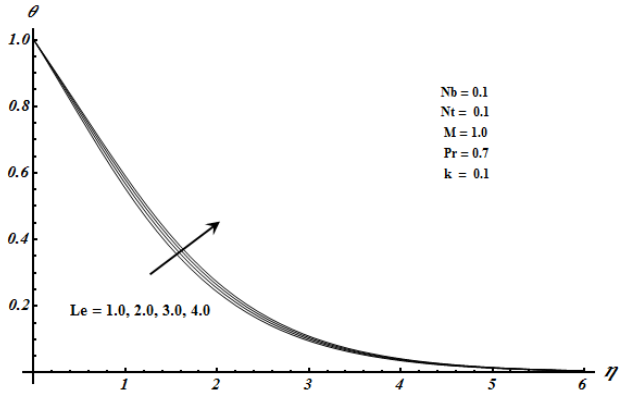

Fig. 12: effects of Le on temperature field $\theta(\eta,t^*)$ when $R(t^*)=1+\varepsilon t^*$, $\varepsilon=0.2$ at $t^*=1$

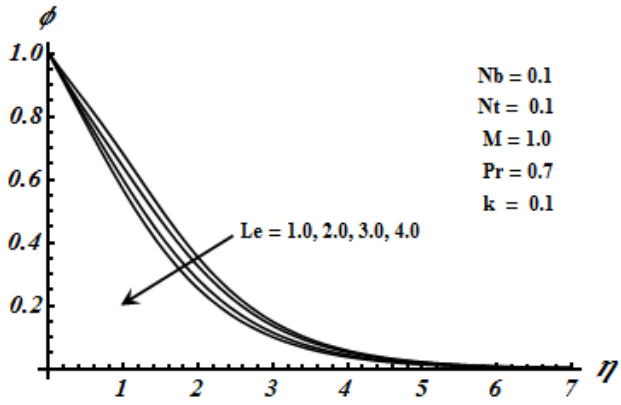

Fig. 13: effects of Le on nano particle volume fraction $\phi(\eta,t^*)$ when $R(t^*)=1+\varepsilon t^*$, $\varepsilon=0.2$ at $t^*=1$

Brownian motion parameter Nb, Thermophoresis parameter Nt and Lewis number Le. The effect of Thermophoresis parameter Nt is to increase the nano particle fraction. The nano particle fraction is a decreasing function of Brownian motion parameter Nb and Lewis number Le. The behavior of temperature profile is opposite for Prandtl number Pr and radiative parameter k. The analytical computation is in acceptable form when comparing with the previous available numerical calculations (see table 3 and 4).

References

[1] R. Hide and P. H Roberts, Pergamon Press, New York, 27–98 (1961).
[2] S. Ostrach and W. H Brown, NACA TN, 4323 (1958).
[3] V. Karman, Uber , ZAMM, **1**, 233–252 (1921).
[4] E. M Sparrow and R. D Cess, Journal of Applied Mechanics, **29**, 181–187 (1962).
[5] M.A Tarek, E.L Mishkawy, A. A Hazem and A. M Adel, Mechanics Research Communications, **25**, 271–278 (1998).

[6] L. A Dorffman, Oliver and Boyd, Edinburgh, (1963).
[7] F. Kreith, Advances in Heat Transfer, **5**, 129–25 (1968).
[8] J. P Hartnett and E. Deland, Journal of Heat Transfer, **83**, 95-96 (1961).
[9] R. G Hering and R. J Grosh,. ASME Journal of Heat Transfer, **85**, 29–34 (1963).
[10] K. Himasekhar, P. K Sarma and K. Janardhan , International Communication in Heat and Mass Transfer, **16**, 99–106 (1989).
[11] N. R Vira and D. N Fan, Journal of Heat Transfer, **103**, 815–817 (1981).
[12] C. Y Wang, Acta Mechnicca, **81**, 245–251 (1990).
[13] M. Alamgir, Transactions of ASME Journal of Heat Transfer, **1**, 174-176 (1976).
[14] H. S Takhar, A. J Chamkha and G. Nath , International Journal of Enggineering Science, **42**, 243–256 (2004).
[15] M. C Ece, Journal of Enggineering Mathematics, **26**, 415–428 (1992).
[16] Roy and D. Anilkumar, International Journal of Heat Mass Transfer, **47**, 1673–1684 (2004).
[17] A. J Chamkha, A. Mudhaf, International Journal of Thermal Science, **44**, 267–276 (2005).
[18] S. Nadeem and S. Saleem, Journal of Taiwan Institute of Chemical Enggineering, **44**, 596–604 (2013).
[19] C. Y Cheng, International Communication in Heat and Mass Transfer, **38**, 44–48 (2011).
[20] S. U. S Choi, Developments and Applications of Non-Newtonian Flows, **66**, 99-105 (1995).
[21] J. A Eastman , S. U. S Choi, L. Li , W. Y and L. J Thompson, Applied Physics Letter, **78**, 718-720 (2001).
[22] A. J Chamkha, R. S. R Gorla and K. Ghodeswar,Transport in Porous Media, **86**, 13–22 (2010).
[23] N. Putra, W. Roetzel and S. K Das, Heat Mass Transfer, **39**, 775–784 (2003).
[24] D. Wen and Y. Ding, IEEE Transactions in Nanotechnology, **5**, 220–227 (2006).
[25] J. Buongiorno, Journal of Heat Transfer, **128**, 241–250 (2006).
[26] R. Ellahi, A. Riaz, S. Nadeem and M. Mushtaq, Applied Mathematics and Infornation Sciences, **7**, 1441-1449 (2013).
[27] R. Ellahi, Applied Mathematics and Modeling, **37**, 1451–1467 (2013).
[28] Noreen Sher Akbar, S. Nadeem and Zafar Hayat Khan, Applied Nanoscience, (2013), 07/s13204-013-0265-2.
[29] Zafar Hayat Khan, W. A Khan, M. Qasim, I. A Shah, IEEE, **99**, 1-9 (2013).
[30] Noreen Sher Akbar, Applied Nanoscience, (2013), 007/s13204-013-0205-1/.
[31] M. Sheikholeslami, R. Ellahi, H. R Ashorynejad, G. Domairry,T. Hayat, Journal of Computational and Theoretical Nanoscience, **11**, 486-496 (2014).
[32] S. J Liao, Chapman & Hall/CRC Press, Boca Raton, (2008).
[33] S. J Liao, Communications in Nonlinear Science and Numerical Simulation, **15**, 2003-2016 (2010).
[34] S. J Liao, Advanced Mechanics, **38**, 1–34 (2008).
[35] S. Abbasbandy, Chemical Engineering Journal, **136**, 144–150 (2008).
[36] R. Ellahi, M. Raza and K. Vafai, Mathematics Computation and Modelling, **55**, 1876–189 (2012).

Sohail Nadeem is an Associate Professor at Quaid-i-Azam University Islamabad. He is recipient of Razi-ud-Din gold medal by Pakistan Academy of Sciences and Tamgha-i-Imtiaz by the President of Pakistan. He is young fellow of TWAS, Italy.

Salman Saleem is working as a PhD Scholar in the department of Mathematics at Quaid-i-Azam University, Islamabad under the supervision of Dr. Sohail Nadeem. He obtained his MS degree with distinction and published his research articles in internationally refereed journals.